Determination of the onset of bulk pinning and the low-temperature-irreversibility line in $Bi_2Sr_2CaCu_2O_{8+\delta}$

C. D. Dewhurst, D. A. Cardwell, A. M. Campbell, and R. A. Doyle
Interdisciplinary Research Centre in Superconductivity, University of Cambridge, West Cambridge Site, Cambridge, CB3 0HE, United Kingdom

G. Balakrishnan and D. McK. Paul
Department of Physics, University of Warwick, Coventry CV4 7AL, United Kingdom
(Received 30 November 1995)

We report the results of dc magnetization measurements of $Bi_2Sr_2CaCu_2O_{8+\delta}$ single crystals as a function of temperature. The evolution of the hysteresis loops with temperature is examined and the irreversibility line extracted. These loops can be scaled onto each other from 4.2 to 20 K, while the lower field part of the loops for the virgin curves continue to scale up to T_c. At intermediate temperatures, the scaling is broken by the appearance of the second peak or ''arrowhead'' which appears at around 20 K but gradually disappears above about 30 K. While the behavior is dominated by significant bulk pinning at low temperatures, the hysteresis and irreversibility fields at high temperatures are considerably modified by geometrical and surface barrier effects. We identify the onset, with increasing field, of bulk pinning and significant critical current from the emergence of the ''arrowhead'' feature from the background surface barrier-determined magnetization curve. Scaling in the low-temperature regime, and extrapolation, enables the irreversibility line at 0 K to be estimated at about 110 T. We propose a phase diagram up to high magnetic fields over a wide range of temperature. [S0163-1829(96)03521-7]

INTRODUCTION

The large anisotropy, unusual parameter values and strong thermal activation effects result in complex vortex behavior and a detailed magnetic phase diagram in high-temperature superconductor (HTS) single crystals.[1] Much experimental attention has focused on the strongly anisotropic $Bi_2Sr_2CaCu_2O_{8+\delta}$ (BSCCO) material where the magnetic phase diagram has variously been investigated by μSR,[2] neutron scattering,[3] superconducting quantum interference device magnetometry,[4] local Hall probes,[5,6] and local inductive probes.[7,8] Recently, theoretical approaches[9] have refocused on the effects of finite electromagnetic coupling between the individual crystallographic CuO_2 layers at the small magnetic inductions where so-called melting and decoupling features have been observed. The importance of this contribution to the elastic moduli of the vortex lattice was originally pointed out by Fisher, Fisher, and Huse[10] and results in the prediction of a re-entrant melting line at low fields, although this has never been observed directly. These studies have, however, stimulated renewed interest in the low-field part of the magnetic phase diagram in BSCCO.

Many measurements performed on single-crystal samples of BSCCO show that the irreversibility line (IL), which defines a field above which pinning effects become insignificant, decreases rapidly with increasing temperature above about 20 K.[11] In some reports the slope of the IL changes almost discontinuously in this regime.[12,13] To date, the behavior of the IL has not been explored systematically above about 12 T which represents the typical field values attainable in modern cryogenic equipment. The low-temperature, high-field regime is of considerable technological interest, since HTS materials potentially offer enhanced magnetic properties under these operating conditions when compared with their conventional LTS counterparts.

In addition to the rapid disappearance of hysteresis in the magnetic moment, well below B_{c2}, with increasing temperature, such measurements on crystals of BSCCO frequently show a double peak in the m-H behavior for fields applied parallel to the c axis.[11,14–17] The second peak, often termed the ''arrowhead,'' is generally observed between 20 and 35 K, and at an applied field of about 40 mT which is almost independent of temperature. This increase in magnetic moment with applied magnetic field has variously been attributed to surface barrier effects,[18] a crossover from surface barrier to bulk pinning,[19] dynamic effects[15,20] or to a three-dimensional to two-dimensional transition in the flux-line structure.[14] The latter is supported by the extreme electrical and magnetic anisotropy of BSCCO which suggests that the behavior normal to the CuO_2 planes is Josephson-like.[11,17–22]

In other words, the material cannot be adequately described by anisotropic three-dimensional (3D) Ginzburg-Landau theory and requires a phenomenology based explicitly on the layered structure of the lattice.

Measurements of the c-axis resistivity ρ_c and c-axis critical current density J_c^c at temperatures above about 40 K in single crystals suggest that the onset of interlayer coupling is dramatically depressed in temperature by the presence of small applied magnetic fields.[23–26] This implies the existence of a 2D vortex structure above a crossover field where interlayer coupling weakens or vanishes. This approximately coincides with the field where the vortices become unpinned. Below about 40 K, although signatures of this dimensional crossover remain at low fields, the irreversibility line rises rapidly and finite critical currents persist to high fields. This is consistent with a strongly pinned quasi-2D vortex lattice. This idea is further supported by the logarithmic flux-creep rate, $S(T)$, which is seen to rise rapidly between 4.2 and 20

K followed by a sharp drop above this temperature.[27–29] Broadly speaking, the field determines the vortex dimensionality, while the temperature determines whether the quasi-2D lattice is pinned or not.

The large electrical and structural anisotropy of single crystals of BSCCO is also reflected in the typical crystal dimensions which are characteristically of the order of mm^2 in the basal plane but only a few tens of μm thick in the c-axis direction. Most magnetic measurements use a field applied normal to the planes to induce shielding currents within the CuO_2 planes in which the superconductivity is thought to reside. This means that the usual measurement geometry is characterized by large demagnetization factors in fields of the order of H_{c1}. A full understanding of the behavior in these low fields is further convoluted by the now well-known surface and geometrical barriers which exist in the transverse geometry for these thin platelets. These effects are particularly pronounced in BSCCO because there is negligible bulk pinning above about 40 K.[13] Above this temperature, the behavior of the vortices is determined by the strong position dependence of their Helmholz free energy and the usual ellipsoidal approximation assumed for this geometry breaks down. As a result the vortices move rapidly to the center of the sample after initial penetration to form a flux pool. The internal field profile is then very different to what is expected from the critical state model and is highly nonuniform. Magnetic hysteresis, and therefore the IL in this regime, is entirely determined by these barrier effects and does not reflect the pinning ability of the sample. Below 40 K bulk pinning starts to become active and a critical state is established at the temperature where the arrowhead feature starts to appear.[13]

An on-going concern is to identify the field and temperature dependence of relative contributions of coupling, pinning and the pronounced geometrical and surface barrier effects on the observed magnetic behavior. Here we have used measurements of the magnetic moment to explore the behavior of BSCCO crystals when a dc field is applied parallel to the c axis. A magnetic phase diagram is constructed and the observed features are discussed in terms of an interplay between coupling, pinning, and geometrical and surface effects.

EXPERIMENTAL

Samples of $Bi_{2.2}Sr_{1.64}Ca_{1.16}Cu_2O_{8+\delta}$ were grown using a traveling floating-zone technique in a double ellipsoidal infrared furnace. Specific details of this method, which produces mosaics of large, aligned crystallites, are given in Ref. 30. The mosaics were repeatedly cleaved until single, optically smooth crystals were obtained. Magnetic moment measurements were carried out on two as prepared crystals with dimensions of 0.6 mm$\times$1.7 mm and thicknesses of between 10 and 20 μm. The T_c of the crystals was measured from the sharp onset of a diamagnetic signal at 89 K. m-H loops were measured in 1 or 2 K temperature intervals between 4.2 and 70 K using an Oxford Instruments VSM3001 vibrating sample magnetometer. The samples were always zero-field cooled before their hysteresis loop was measured. The remnant field in the magnet was reduced to below 1 mT between each run by oscillating the magnet field sinusoidally while reducing the amplitude of the oscillations. The magnetic field was applied parallel to the c axis of the crystals and swept to 12 T, or to a value greater than the temperature-dependent irreversibility field determined using a criterion of $\Delta M = 5\times10^{-9}$ A m^2 ($J_c = 100$ A/cm^2). The behavior at sweep rates of 0.5 and 10 mT/s was measured in each case to ensure that creep in the sample had no qualitative effect on our conclusions, although this effect was not studied in detail here.

RESULTS AND DISCUSSION

We begin with a discussion of the m-H behavior of the crystals at low temperatures where bulk pinning is well established. In this regime, the magnetic hysteresis at any given applied field increases (exponentially) with decreasing temperature and plots of curves between 4.2 and 16 K on the same axes are not very informative. On the other hand, the m-H loops are very similar in form when plotted individually and show a monotonic decrease in moment for fields greater than the low-field peak close to full penetration.

This suggests that the magnetic moment may obey some general scaling behavior, being determined by the same underlying physical mechanisms. Indeed the curves coincide almost exactly when their field and moment axes are normalized by the field, $H^*(T)$ and the moment, $m^*(T)$, which corresponds to the first penetration peak. This scaled data is presented for several temperatures between 4.2 and 16 K in Fig. 1. The significance of scaling parameters for magnetization measurements of HTS crystals has been discussed in detail in Refs. 31 and 32 and is also a central concern of this paper. $H^*(T)$ indicates the field at which the magnetization curve exhibits a maximum diamagnetic signal and is significantly larger than H_{c1} because of finite-pinning effects which resist entry of flux.[33] Both $H^*(T)$ and $m^*(T)$ contain information about J_c and the pinning force density of the sample at fields close to that of full penetration.

Figure 1(b) shows m-H curves at higher temperatures, also scaled to the penetration peak parameters, but in the temperature range between 16 and 24 K. The coincidence of the curves is reduced significantly, especially for the decreasing field cycle. This suggests that the physical process which determines the magnetic hysteresis at lower temperatures begins to change in this temperature regime. In addition, anomalous features begin to appear in the m-H curves at fields close to, but higher than, $H^*(T)$. It is clear that the failure of the scaling is most pronounced above the onset of this anomaly which suggests that these two observations are related. This is confirmed in Fig. 1(c) where similarly scaled m-H curves are shown at temperatures between 23 and 30 K. The low-field part of the loops below the anomaly scale very well to the (first) peak parameters, after which the scaling breaks down significantly and systematically. It may be assumed, therefore, that the first peak parameters have a different origin to those in the 4.2–16 K regime at these higher temperatures. As pinning effects become negligible, $H^*(T)$ begins to approximate the field for first penetration $H_p(T)$. It is tempting to rescale the curves to the field, $H^{*\prime}(T)$, and moment, $m^{*\prime}(T)$, associated with the arrowhead or second peak in the higher-temperature regime. Such a rescaling does not yield coincident curves, however, as shown in Fig. 1(d).

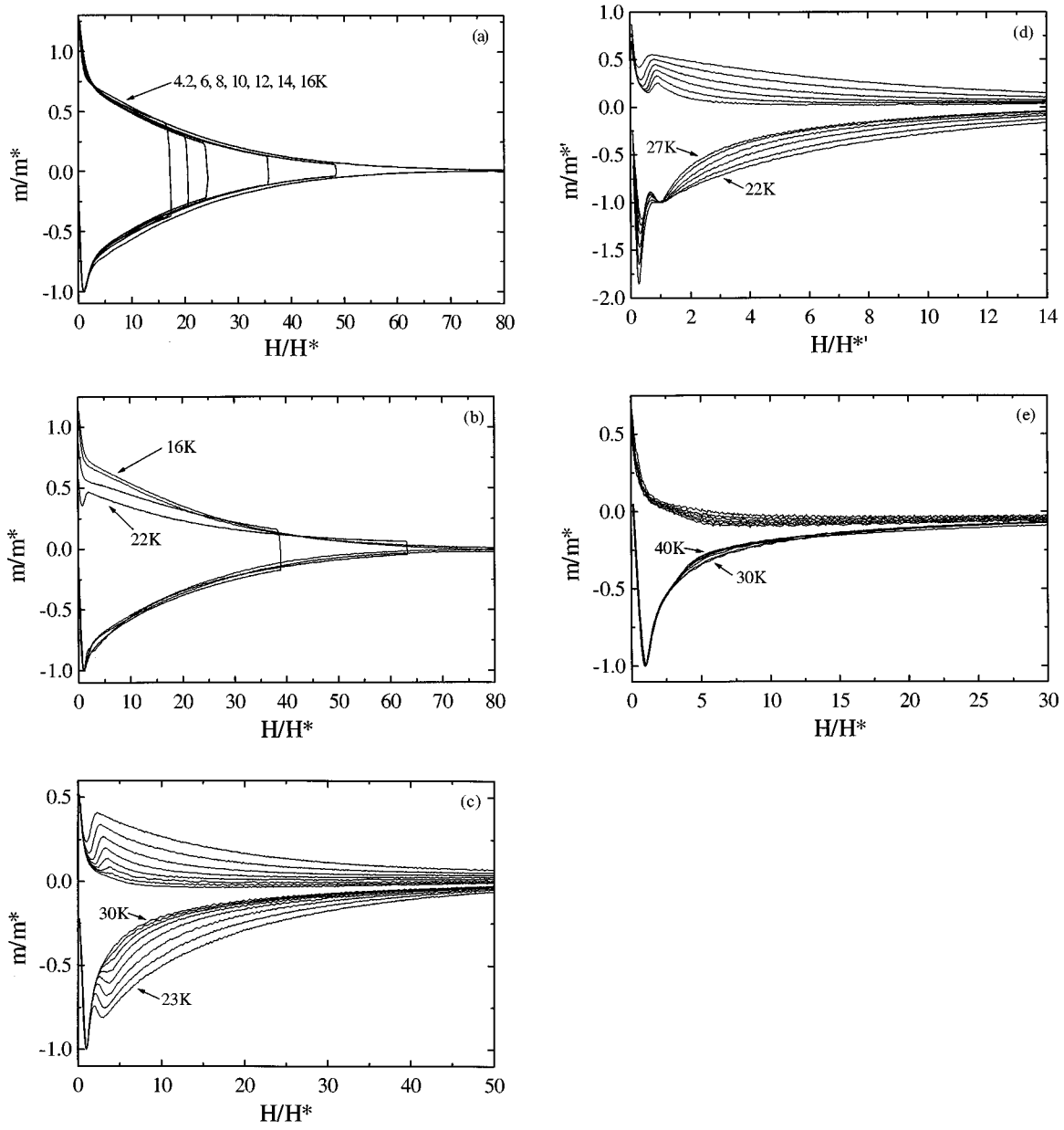

FIG. 1. Scaled m-H curves at temperatures between 4.2 and 40 K. (a), (b), (c), and (e) are scaled to the parameter $[H^*(T), m^*(T)]$. (d) is scaled to the arrowhead peak anomaly $[H^{*\prime}(T), m^{*\prime}(T)]$.

Figure 1(e) shows higher-temperature hysteresis loops from 30 to 40 K again scaled to the penetration peak parameters, $H^*(T)$ and $m^*(T)$. The arrowhead feature, which was prominent between 22 and 30 K has clearly now disappeared and the data appears to scale reasonably well again, at least on the ascending field cycle. Asymmetry in the m-H loop is important evidence for discriminating between pinning and surface and geometrical barrier induced hysteresis, since pinning always produces symmetric hysteresis. Although we have not presented data for higher temperatures, it is clear that the moment on the decreasing field cycle becomes increasingly parallel to the field axis with increasing temperature. This is in agreement with what is expected as the last vestiges of pinning disappear and the behavior becomes entirely determined by geometrical and surface barriers. Nevertheless it is apparent that the low-field part of the virgin curve continues to scale. The IL is also now obviously determined not by reversibility due to thermally activated depinning but rather by the detailed manner in which the reverse leg flattens with increasing temperature as the irreversible magnetization is increasingly determined by surface rather than bulk currents.

We now begin construction of a phase diagram, starting with the irreversibility field at which magnetic hysteresis disappears. The factors which determine this in the various temperature windows defined in Figs. 1(a)–1(e) are the basis of the following discussion. The IL is determined from the disappearance of hysteresis in the measured m-H loops using a criterion of 5×10^{-9} A m^2 (this corresponds to a J_c of 100 A/cm^2 for our sample geometry). The temperature dependence of the irreversibility field is shown on linear and log scales in Figs. 2(a) and 2(b), respectively. Clearly, it is not

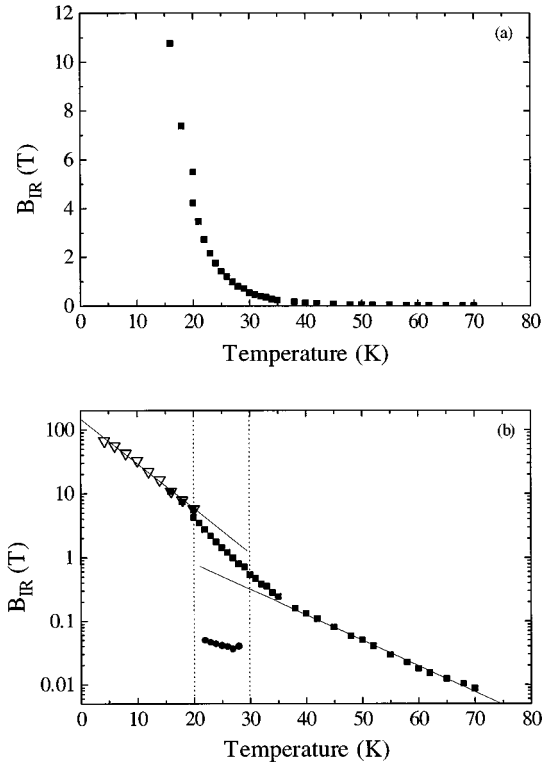

FIG. 2. (a) Irreversibility line as measured from the point of hysteresis closure. (b) measured (solid squares) and scaled (open triangles) irreversibility line. The solid lines are a guide for the eye and indicate regions where the irreversibility line varies exponentially with temperature. Also shown is the arrowhead peak position (solid circles) on the ascending side of the hysteresis loop. The region bounded by the dotted lines indicates the crossover region between the two exponential regimes of the irreversibility line.

possible to extract the irreversibility field when it lies above the maximum field that can be applied with the superconducting solenoid. However, the scaling behavior in Fig. 1(a) suggests that the magnetic moment, and therefore the irreversibility fields, are self-similar between 4.2 and 16 K. We use this observation to extrapolate the irreversibility field beyond the measurable range using the scaling parameters obtained from the penetration peak. These extrapolated values are included as open triangles in Fig. 2(b). The form of the IL is identical to that reported elsewhere[13,34–36] for high-quality BSCCO crystals for $B\|c$, and is characterized by a rapid increase in the irreversibility field below about 20 K. The irreversibility line deduced from the m-H data at 4.2 K scaled to the field, $H^*(T)$, yields a value of $\mu_0 H_{\rm IL}$ (4.2 K)=67 T. The low-temperature behavior of the IL is important since the behavior of H_{c2} at low temperatures is still controversial in HTS and since the quantum number in these systems is such that one might expect significant effects of quantum creep.[1] Although no m-H data were measured below 4.2 K, a sufficiently large number of IL(T) data points in the low-temperature regime were extracted in order to speculate about the value of $H_{\rm IL}$ (0 K). The curve in Fig. 2(b) below about 10 K appears to have negative curvature rather than the upward curvature displayed by H_{c2} data in Ref. 37, indicating that $H_{\rm IL}$ saturates at 0 K. Fitting a second-order polynomial to this data yields a value of about 110 T for $\mu_0 H_{\rm IL}$ (0 K). This value is considerable larger than early

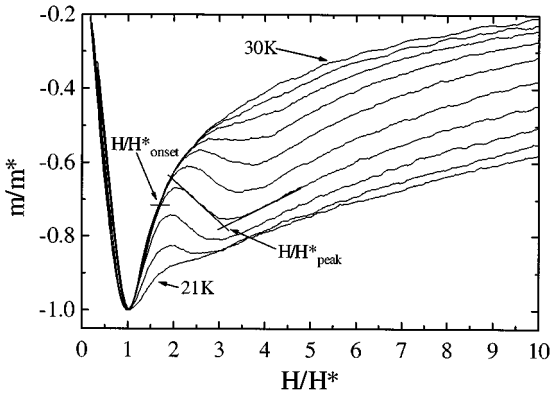

FIG. 3. Bulk pinning becomes active at some characteristic reduced field $H/H^*_{\rm onset}$. The arrowhead anomaly grows outwards from a background m-H curve dominated by geometrical and surface effects, reaching a maximum at a reduced field $H/H^*_{\rm peak}$.

estimates of H_{c2} (0 K), which predict $\mu_0 H_{c2}$ (0 K)=44 T calculated from $\xi_{\rm ab}$ (0 K)=38 Å.[38] However this number is considerably smaller than the estimate of $\mu_0 H_{\rm IL}$ (0 K)=492 T by Indenbom *et al.*, obtained from an exponential fit to the IL determined by torque measurements at intermediate temperatures.[35] Figure 2(b) shows that there are three distinct regions in the IL at low, intermediate, and high temperatures. The behavior is exponential at very low and at the highest temperatures as indicated by the linear fits to the data in these regimes. There is a crossover between these ranges which also appears to be exponential although this may be an artefact of more than one mechanism determining the measured behavior. It is important to note that the arrowhead anomaly is observed only within the crossover region which is bounded by the dotted lines.

Next we present a discussion of the factors which determine the arrowhead feature. It is clear from a comparison of Figs. 1(c) and 1(e) that the m-H behavior below the arrowhead field is similar to that at all fields at higher temperatures. This is apparent from Fig. 3 where the data shown in Fig. 1(e) is presented on an expanded scale for the increasing field cycle only, at temperatures between 21 and 30 K. The arrowhead feature appears to grow, at some characteristic reduced field $H/H^*_{\rm onset}$, out of a background curve determined by some other mechanism. An increase in magnetic moment is usually ascribed to a field-dependent increase in critical current and this type of peak effect may occur from one of two mechanisms. The first involves a matching effect where one has a well defined system of pinning sites and the applied field is such that all pinning sites pin one vortex. The other type of peak effect usually appears close to B_{c2} and results from a softening of the vortex lattice which increases collective pinning, thereby increasing J_c. Yang *et al.*[14] have suggested that a matching effect due to dislocations in BSCCO may be responsible for the arrowhead. However this suggestion is inconsistent with earlier reports of Chikumoto *et al.*[39(a),(b)] who investigated the effects of electron irradiation on this feature. They show that the effect of electron damage is to reduce the field at which the arrowhead is observed, contrary to what is expected from a matching effect. They conclude that the arrowhead is indeed caused by an increase in J_c but have not addressed the underlying mechanism for this increase in detail.

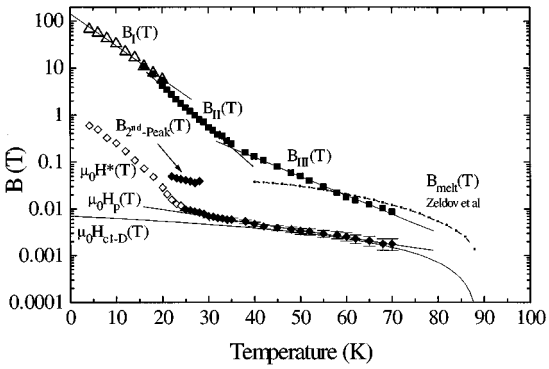

FIG. 4. Magnetic phase diagram as constructed from our magnetization data. The measured and scaled irreversibility lines are indicated by the solid square and open triangle symbols, respectively. The solid lines labeled $B_{\mathrm{I}}(T)$, $B_{\mathrm{II}}(T)$, and $B_{\mathrm{III}}(T)$ are a guide for the eye and indicate the three near exponential regimes of the irreversibility line. The scaling parameter $\mu_0 H^*(T)$ is denoted by open diamonds at low temperatures and by solid diamonds at high temperatures when $H^*(T)$ approximates the penetration field $H_p(T)$. The solid line through $\mu_0 H_p(T)$ is a guide for the eye and indicates the exponential dependence expected for a thermally activated surface barrier. The solid line denoted by $\mu_0 H_{c1-D}(T)$ is a fit of $H_{c1}(T)=H_{c1}(0)D(1-T/T_c)$ where $H_{c1}(0)=25.3$ mT (Ref. 13) and $D=0.4$. Also shown is the arrowhead peak position denoted by $B_{\mathrm{2nd\text{-}peak}}(T)$ (solid diamonds) and the melting line as reported by Zeldov *et al.* (Ref. 5) (dot-dashed line).

Recently, Zeldov *et al.*[13] have provided further support, from local Hall probe measurements, for the observations of Chikumoto.[39(a)] These indicate strongly that a critical state is only established above the arrowhead feature and that the behavior at lower fields is determined largely by geometrical barriers.[6,13] This interpretation is also supported by our global magnetization measurements. Although we cannot directly measure the field profiles within our sample, a scaling approach has been used to identify regions of field and temperature within which the behavior is determined by a single mechanism. The onset of different types of behavior can then be used to identify crossovers or transitions in the phase diagram. A reasonable phenomenological explanation for the increase in J_c at the arrowhead may be based on the weak Josephson coupling between the CuO_2 layers. An abrupt field-dependent softening of the vortex tilt modulus, C_{44}, and loss of topological longitudinal correlation of a 3D vortex lattice would result in a decrease in the vortex correlation volume. In the picture provided by collective-pinning theory[40] this would result in an increase in J_c. This explanation is also supported by neutron scattering[3] and μSR (Ref. 2) data. A detailed analysis of the field dependence in the vicinity of the arrowhead, including creep effects, will be presented in Ref. 41. Finally we note that a temperature-independent decoupling field is theoretically difficult, since all decoupling or melting scenarios in 2D systems predict a vertical line in the B-T phase field.

It is now possible to construct a magnetic phase diagram for BSCCO from Figs. 1–3. This is shown in Fig. 4 on a logarithmic field scale. The uppermost locus described by the measured data points, which are the same as for the IL shown in Figs. 2(a) and 2(b) has now been divided into three lines, $B_{\mathrm{I}}(T)$, $B_{\mathrm{II}}(T)$, and $B_{\mathrm{III}}(T)$. The basis of these distinctions are described as follows. The low-temperature data denoted by $B_{\mathrm{I}}(T)$ is the irreversibility data extracted from our scaling analysis and has not been reported previously. The intermediate-temperature regime of the IL, denoted in Fig. 4 by B_{II}, also appears to have an almost exponential behavior as observed by other groups on the basis of magnetic torque and transport measurements.[35,36] The IL is exponential at high temperatures where it is now clear that the behavior $B_{\mathrm{III}}(T)$ is determined by geometrical or surface barriers rather than activation of a weak, random pinning array. This has also been shown by Zeldov *et al.*,[13] Chikumoto,[39(a)] and Indenbom *et al.*[35] from local magnetic, third-harmonic generation, and magneto-optical measurements, respectively. An elegant proof for this has recently been shown by Majer, Zeldov, and Konczykowski who polished a rectangular crystal into a prism, thereby removing the geometrical barriers and substantially reducing the IL.[42] This caused the material to become completely reversible above 76 K. The solid lines through $B_{\mathrm{I}}(T)$, $B_{\mathrm{II}}(T)$, and $B_{\mathrm{III}}(T)$ are fits to the function $B_{\mathrm{IL}}(T)=B_{\mathrm{IL0}}\exp(T/T_0)$. These yield the parameters given in Table I.

TABLE I. Exponential fit parameters to the irreversibility data given in Fig. 4.

IL	B_{II0} (T)	T_0 (K)
B_{I}	147	6.21
B_{II}	222	4.98
B_{II}	5.15	10.77

Although we have been unable to observe any signature of a first-order melting and/or decoupling behavior recently reported from local measurements on BSCCO,[6–8] it is appropriate to include these on the phase diagram. The dot-dashed line in Fig. 4 at high temperatures indicates the first-order transition data reported by Zeldov *et al.*,[5] which can be seen to cross the IL at about 58 K and 30 mT. It has now been shown that the first-order transition always runs into the arrowhead field at low temperatures,[6,43] to form a continuous locus. This is so even when both transitions are systematically shifted by changing the oxygen doping, and therefore the anisotropy in the material. It is most important to identify what happens to this line at low temperatures since a field-independent transition cannot easily be reconciled with either melting or decoupling theories. In order to investigate this further, we have included our scaling parameter $\mu_0 H^*(T)$ in Fig. 4. Below about 30 K, $H^*(T)$ deviates significantly from the exponential behavior observed at higher temperatures and the closed diamonds have been replaced with open diamonds. Here $H^*(T)$ rises rapidly with decreasing temperature because of rapidly increasing bulk pinning. It is evident that there is a clear change in $H^*(T)$ as well as the IL at about 20 K and that this is the temperature where the arrowhead feature disappears into the pinning controlled penetration peak. μSR studies suggest that a 3D to 2D transition at around 40 mT in optimally doped BSCCO, persists right down to 4.2 K although this cannot be resolved in the data presented here due to pinning.

Finally we discuss the temperature range between 30 and about 70 K, where $H^*(T)$ varies exponentially. A very similar behavior was observed by Zeldov *et al.*[13] There they use

an exponential fit,[44] given by $H_p(T)=H_{p0}\exp(-T/T_0)$. A fit of this expression to $\mu_0 H^*(T)$ is indicated by the solid line in Fig. 4 for temperatures greater than 30 K. This yields values for the fitting parameters of $\mu_0 H_{p0}=19$ mT and $T_0=29.34$ K which are in close agreement with similar values quoted in Refs. 13 and 44. A detailed discussion of this behavior is presented in Ref. 41. At temperatures close to T_c, $\mu_0 H^*(T)$ is expected to approach the field for first penetration $H_{c1}(T)$, corrected for demagnetization effects as also shown in Ref. 13. We fit the high-temperature data for $\mu_0 H^*(T)$ with the function $H_{c1}(T)=H_{c1}(0)D(1-T/T_c)$ using a value of $\mu_0 H_{c1}(0)=25.3$ mT,[13] where D is a constant related to the geometry-dependent demagnetization factor and the geometrical barrier. We deduce a value for D of about 0.3 for our crystal. This fit is marked by the solid line in Fig. 4 denoted by $\mu_0 H_{c1-D}(T)$.

CONCLUSIONS

We have proposed a phase diagram for BSCCO for the entire range of temperatures below T_c and for applied fields from 1 mT to 100 T. Each part of the phase diagram is consistent with other published data which has focused on individual features in the B-T diagram. In particular, we have shown that scaling of the magnetic moment allows many features previously thought to be apparent only in the local magnetization (due to the geometrical and surface barriers) to be identified from global magnetization measurements over a wide field and temperature range. This approach has also allowed us to estimate the low-temperature, high-field irreversibility line and to show the clear development of a critical current with increasing field in the vicinity of the arrowhead feature.

ACKNOWLEDGMENTS

We would like to thank E. Zeldov for allowing us access to preprints. We would also like to thank L. F. Cohen and G. K. Perkins for many useful discussions. We are grateful for the financial support of a Girton College Research Fellowship (RAD) and an EPSRC CASE award sponsored by MagneTek Ltd. (CDD).

[1] G. Blatter, M. V. Feigelman, V. B. Geshkenbein, A. I. Larkin, and V. M. Vinokur, Rev. Mod. Phys. **66**, 1125 (1994).
[2] S. Lee, M. Warden, H. Keller, J. W. Schneider, D. Zech, P. Zimmermann, R. Cubitt, E. M. Forgan, M. T. Wylie, P. H. Kes, T. W. Li, A. A. Menovsky, and Z. Tarnawski, Phys. Rev. Lett. **75**, 922 3862 (1993).
[3] R. Cubitt, E. M. Forgan, G. Yang, S. L. Lee, D. McK. Paul, H. A. Mook, M. Yethiraj, P. H. Kes, T. W. Li, A. A. Menovsky, Z. Tarnawski, and K. Mortensen, Nature (London) **365**, 407 (1993).
[4] H. Pastoriza, M. F. Goffman, A. Arribere, and F. de la Cruz, Phys. Rev. Lett. **72**, 2951 (1994).
[5] E. Zeldov, D. Majer, M. Konczykowski, V. B. Geshkenbein, V. M. Vinokur, and H. Strikman, Nature (London) **375**, 373 (1995).
[6] B. Khaykovich, E. Zeldov, D. Majer, T. W. Li, P. H. Kes, and M. Konczykowski (unpublished).
[7] Y. Ando, S. Komiya, Y. Kotaka, and K. Kishio, Phys. Rev. B **52**, 3765 (1995).
[8] R. A. Doyle, D. Liney, W. S. Seow, A. M. Campbell, and K. Kadowaki, Phys. Rev. Lett. **75**, 4520 (1995).
[9] G. Blatter, M. V. Feigel'man, V. B. Geshkenbein, A. I. Larkin, and V. M. Vinokur, Rev. Mod. Phys. **66**, 1125 (1994).
[10] D. Fisher, M. P. A. Fisher, and D. A. Huse, Phys. Rev. B **43**, 130 (1991).
[11] K. Kishio, J. Shimoyama, Y. Kotaka, and K. Yamafuji, in *Proceedings of the 7th International Workshop on Critical Currents, Alpbach, Austria*, edited by Harald H. Weber (World Scientific, Singapore, 1994), p. 339.
[12] H. Pastoriza, F. de la Cruz, D. B. Mitzi, and A. Kapitulnik, Phys. Rev. B **46**, 9278 (1992).
[13] E. Zeldov, D. Majer, M. Konczykowski, A. I. Larkin, V. M. Vinokur, V. B. Geshkenbein, N. Chikumoto, and H. Shtrikman, Europhys. Lett. **30**, 367 (1995).
[14] G. Yang, P. Shang, S. D. Sutton, I. P. Jones, J. S. Abell, and C. E. Gough, Phys. Rev. B **48**, 4054 (1993).
[15] Y. Yeshurun, N. Bontemps, L. Burlachov, and A. Kapitulnik, Phys. Rev. B **49**, 1548 (1994).
[16] G. Yang, J. S. Abell, and G. E. Gough, in *Proceedings of the 7th International Workshop on Critical Currents, Alpbach, Austria* (Ref. 11), p. 264.
[17] S. Ryu, S. Doniach, G. Deutscher, and A. Kapitulnik, Phys. Rev. Lett. **68**, 710 (1992).
[18] V. N. Kopylov, A. E. Koshelev, I. F. Schegolev, and T. G. Togonidze, Physica C **170**, 291 (1990).
[19] N. Chikumoto, M. Konczykowski, N. Motihira, and A. P. Malozemoff, Phys. Rev. Lett. **69**, 1260 (1992).
[20] L. Krusin-Elbaum, L. Civale, V. M. Vinokur, and F. Holtzberg, Phys. Rev. Lett. **69**, 2280 (1992).
[21] T. Tamegai, Y. Iye, I. Oguro, and K. Kishio, Physica C **223**, 33 (1993).
[22] J. R. Clem, Phys. Rev. B **43**, 7837 (1991).
[23] J. H. Cho, M. P. Maley, S. Fleshler, A. Lacerda, and L. N. Bulaevskii, Phys. Rev. B **50**, 6493 (1994).
[24] S. N. Gordeev, W. Jahn, A. A. Zhukov, H. Kupfer, and A. A. Bush, in *Proceedings of the 7th International Workshop on Critical Currents, Alpbach, Austria* (Ref. 11), p. 165.
[25] M. C. Hellerqvist, S. Ryu, L. W. Lombardo, and A. Kapitulnik, Physica C **230**, 170 (1994).
[26] K. Kadowaki, T. Mochiku, H. Takeya, Y. Saito, and K. Hirata, J. Superconduct. **8**, 461 (1995).
[27] V. V. Metlushko, G. Guntherodt, I. N. Goncharov, A. Yu. Didyk, V. V. Moshchalkov, and Y. Bruynseraede, Physica B **194–196**, 2219 (1994).
[28] V. V. Metlushko, G. Guntherodt, V. V. Moshchalkov, and Y. Bruynseraede, Europhys. Lett. **26**, 371 (1994).
[29] V. N. Zavaritsky, *Electronic Properties and Mechanisms of High T_c Superconductors* (Elsevier, Amsterdam, 1992), p. 367.
[30] G. Balakrishnan, D. Mc. Paul, M. R. Lees, and A. T. Boothroyd, Physica C **206**, 148 (1993).
[31] G. K. Perkins, L. F. Cohen, A. A. Zhukov, and A. D. Caplin, Phys. Rev. B **51**, 8513 (1995).
[32] A. A. Zhukov, H. Kupfer, V. A. Ryachuck, L. A. Ponomarenko, V. A. Murashov, and A. Yu. Martynkin, Physica C **219**, 99 (1994).

[33] C. P. Bean, Rev. Mod. Phys. **36**, 31 (1964).
[34] E. Zeldov, A. I. Larkin, V. B. Geshkenbein, M. Konczykowski, D. Majer, B. Khayovich, V. M. Vinokur, and H. Strikman, Phys. Rev. Lett. **73**, 1428 (1994).
[35] M. V. Indenbom, G. D'Anna, M. O. Andre, W. Benoit, H. Kronmuller, T. W. Li, and P. H. Kes, in *Proceedings of the 7th International Workshop on Critical Currents, Alpbach, Austria* (Ref. 11), p. 327.
[36] V. N. Zavaritsky (private communication).
[37] A. P. MacKenzie, S. R. Julian, A. Carrington, G. G. Lonzarich, D. J. C. Walker, J. R. Cooper, and D. C. Sinclair, Physica C **235**, 233 (1994).
[38] T. T. M. Palstra, B. Batlogg, L. F. Scneemeyer, R. B. van Dover, and J. V. Waszczak, Phys. Rev. B **38**, 5102 (1988).
[39] (a) N. Chikumoto, Ph.D. thesis, University of Tokyo, 1993; (b) N. Chikumoto, M. Konzcykowski, N. Motohira, K. Kishio, and K. Kitazawa, Physica C **185-189**, 2201 (1991).
[40] A. I. Larkin and Y. N. Ovchinnikov, J. Low Temp. Phys. **34**, 409 (1979).
[41] L. F. Cohen *et al.* (unpublished).
[42] D. Majer, E. Zeldov, and M. Konczykowski, Phys. Rev. Lett. **75**, 1167 (1995).
[43] T. Hanaguri, T. Tsuboi, A. Maeda, T. Nishzaki, N. Kobayashi, Y. Kotaka, J. Shimoyama, and K. Kishio, Physica C **256**, 11 (1996).
[44] L. Burlachkov, V. B. Geshkenbein, A. E. Koshelev, A. I. Larkin, and V. M. Vinokur, Phys. Rev. B **50**, 16 770 (1994).